Aspects of the anodic behaviour of duplex stainless steels aged for long periods at low temperatures

J.E. May [a], C.A.C. de Sousa [b], S.E. Kuri [a,*]

[a] *DEMa, Federal University of São Carlos, Rod Washinton Luis, km 235, C. Postal 676, 13565-905 São Carlos, SP, Brazil*
[b] *DCTM, Federal University of Bahia, 40.110-060 Salvador, BA, Brazil*

Abstract

Duplex stainless steel samples were aged at low temperatures (300 and 400 °C) for 1000 and 2000 h. Their anodic behaviour was studied in a 0.1 N concentration of sulphuric acid, which revealed that the polarisation curves were dependent on the aging temperature and time. Complex anodic current peaks occurred at low and high potentials due to the dual austenite and ferrite microstructure. The aging treatment promoted silicon enrichment of the passivated film, probably over the austenite phase, as indicated by X-ray photoelectron spectroscopy measurements. G phase precipitation and spinodal decomposition was identified by transmission electron microscopy.
© 2003 Elsevier Science Ltd. All rights reserved.

1. Introduction

Duplex stainless steels (DSSs) are used in a wide variety of applications, combining good corrosion resistance, weldability, good castability and high mechanical strength. They are little susceptible to stress corrosion cracking and intergranular corrosion, and possess a high pitting corrosion resistance. DSSs have been used increasingly as structural materials in various applications that require high mechanical strength and in highly corrosive environments such as chemical plants,

---
* Corresponding author. Tel.: +55-16-260-8244; fax: +55-16-261-5404.
E-mail address: dsek@power.ufscar.br (S.E. Kuri).

offshore installations, thermal power plants, etc. They are prime candidates for sour well applications where H_2S, CO_2 and chlorides are found [1–3].

The properties of DSSs arise from an equilibrium of the austenitic (γ) and ferritic (α) phases obtained by either chemical composition or thermal treatment and its best properties are achieved with a 50:50 α/γ ratio.

DSSs are susceptible to the formation of additional phases that can influence their mechanical and corrosion properties. These phases correspond to the precipitation of various compounds such as chromium carbides, nitrides and several other intermetallic phases. These phases can be formed during solidification, subsequent heat treatment, or by plastic deformation or aging during their service life [2]. As an example, pipes used in primary coolant water in pressurised nuclear reactors are designed for a 40-year service life and their long-term mechanical and corrosion integrity are of the utmost importance for safe operation. However, aging during service in some temperature ranges can degrade the material's mechanical and corrosion properties [3]. Long-term thermal aging in the range of 300–400 °C produces an increase in hardness and tensile properties, together with a decrease in the impact properties, ductility and toughness. Earlier studies [4,5] have attributed such degradations of mechanical properties to a spinodal reaction occurring in the ferrite phase, in which the ferrite decomposes into an iron-rich phase and an enriched chromium α' phase [6], but other precipitated phases, such as a complex nickel silicide known as G phase, have also been observed [3]. In the 700–1000 °C range, increased contents of Cr, Ni and Mo in the steel composition accelerate the precipitation of a σ-phase and other precipitates (nitrides, χ-phase), which have a strong negative impact on corrosion resistance [4]. When chromium precipitation occurs, depleted areas cause reductions in the corrosion resistance [6]. Moreover, the appearance of the σ-phase is also a ductility-reducing factor [2].

Therefore, despite several studies about the effect of phase precipitation on DSS properties, there is little information about DSS performance in the presence of precipitation at low temperatures, particularly about its corrosion properties. In this study, an analysis was made of the corrosion properties and passivation of DSS with high chromium content after long-term aging (1000 and 2000 h) at 300 and 400 °C.

2. Experimental procedures

The samples used in this investigation were obtained from a hot rolled DSS whose composition is given in Table 1.

The samples were aged in a horizontal electric furnace for 1000 and 2000 h at two different temperatures (300 and 400 °C) and then quenched in water at 25 °C.

Table 1
Chemical composition of the DSS, wt.%

C	Cr	Ni	Mo	Cu	Mn	Si	P
0.11	29.4	8.70	0.08	0.10	1.77	0.41	0.02

The effect of aging on the susceptibility to intergranular corrosion was assessed by the ''double loop reactivation method'' [9] and polarisation curves were obtained by potentiodynamic polarisation methods.

The work electrodes used for testing by the polarisation technique consisted of cylindrical samples insulated by an epoxy resin, polished with 600 grade silicon carbide paper, rinsed in alcohol and dried before each measurement. A platinum counter electrode was used and the reference electrode consisted of a saturated calomel electrode, to which all potentials are related. The working solution (0.1 N H_2SO_4) was prepared from distilled water and analytical grade sulphuric acid. The potentiodynamic polarisation curves were determined using a PAR model 370 electrochemical system at a 10-mV/s-scan rate.

X-ray photoelectron spectroscopy (XPS) was used to analyse the surface with a Kratos XSAM HS spectrometer, using Mg K_α radiation, 1253.6 eV energy, 15 kV power and 5 mA emission. The background was subtracted by the Shirley method [7] and the peaks were fitted using both Gaussian and mixed Gaussian/Lorentzian functions [8].

3. Results and discussion

Fig. 1 shows the microstructure of two samples, the first in the unmodified condition (Fig. 1a) and the second (Fig. 1b) aged at 400 °C for 2000 h. No microstructural change was observed by optical microscopy analysis during long-term aging, since only austenite and ferrite appeared in the two microstructures.

Substantial phase precipitation was detected when the samples were analysed by transmission electron microscopy. The double loop reactivation method, however, showed that this fine precipitation was insufficient to induce significant susceptibility to intergranular corrosion, as illustrated in Fig. 2. A tendency for reactivation with a very low anodic current was observed during sweeping in the cathodic direction. With this method, when the ratio of peak current in the anodic direction to peak current in the cathodic direction increases, the degree of sensitisation also increases.
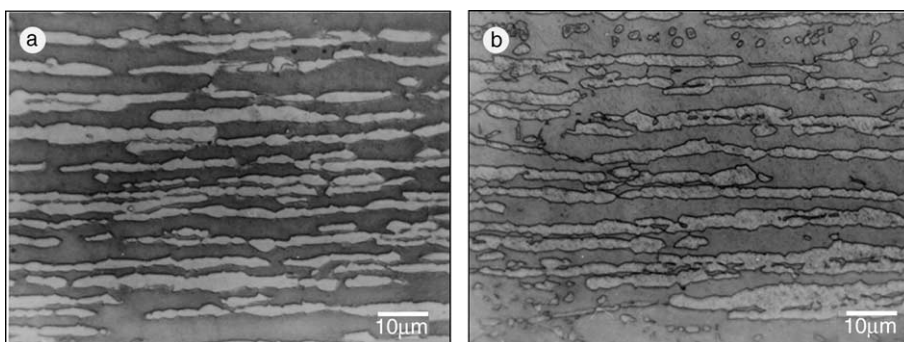
Fig. 1. DSS microstructure: (a) unmodified condition, (b) aged at 400 °C for 2000 h.
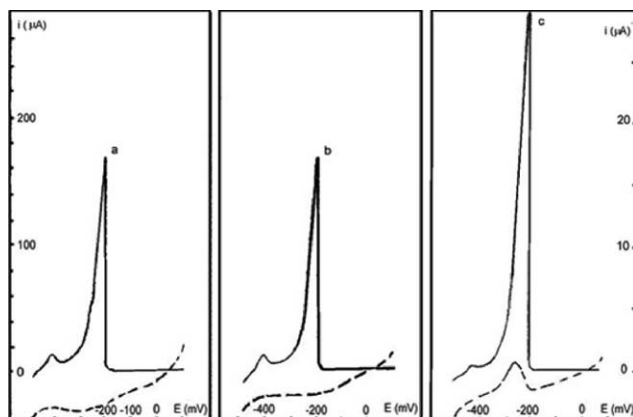
Fig. 2. Results obtained from the double loop reactivation method for samples aged at 400 °C for 2000 h, showing a reactivation peak: (a) unaged; (b) aged for 1000 h at 400 °C; (c) aged for 2000 h at 400 °C.

Some authors [11] consider the material to be sensitised steel when this ratio lies in the range of 7.0×10^{-3}. Considering the results shown in Fig. 2, which indicate a peak current ratio of 3.0×10^{-3}, it appears that only the samples aged at 400 °C for 2000 h became partially sensitised, while the remaining samples showed no reactivation peak.

Aging treatment changed the polarisation curves drastically, particularly in the passivation and transpassivation regions. Fig. 3 shows anodic potentiodynamic polarisation curves in the region of low potential (Fig. 3a) and in the region of high potential (Fig. 3b). These polarisation curves indicate two potentials in which a complex current peak occurred. Each of these complex peaks can be considered an overlapping of two simple current peaks. In the low potential region, the peaks are present at ≈ -405 mV (peak $E_{1\alpha}$) and -307 mV (peak $E_{1\gamma}$), while the high potential region shows peaks at $+1250$ mV (peak $E_{2\alpha}$) and $+1344$ mV (peak $E_{2\gamma}$). According to Symniotis [5], this may be attributed to the DSS's dual phase ferrite/austenite microstructure, which gives rise to galvanic action that accelerates the selective dissolution of the ferrite phase. The peak occurring at $E_{1\alpha}$ corresponds to the dissolution and passivation of the ferrite phase and the peak at $E_{1\gamma}$ corresponds to the dissolution and passivation of the austenite phase. The complex peak at higher potentials is related to transpassive dissolution and to a secondary passivation (due to a stoichiometric transformation of the passivated film) occurring in the ferrite phase at $E_{2\alpha}$ and in the austenite phase at $E_{2\gamma}$, both with simultaneous oxygen evolution.

To support the argument for secondary passivation, Fig. 4 indicates the results of a chronoamperometry experiment conducted at $E_{2\alpha}$ and $E_{2\gamma}$. As can be seen, the current continuously decreases at both potentials, but with stronger kinetic decay in the austenite phase. This demonstrates that the secondary passivation, caused by the stoichiometric transformation of the passivated film, occurs faster in the austenite phase than in the ferrite phase (probably due to the high silicon content in the austenite phase).
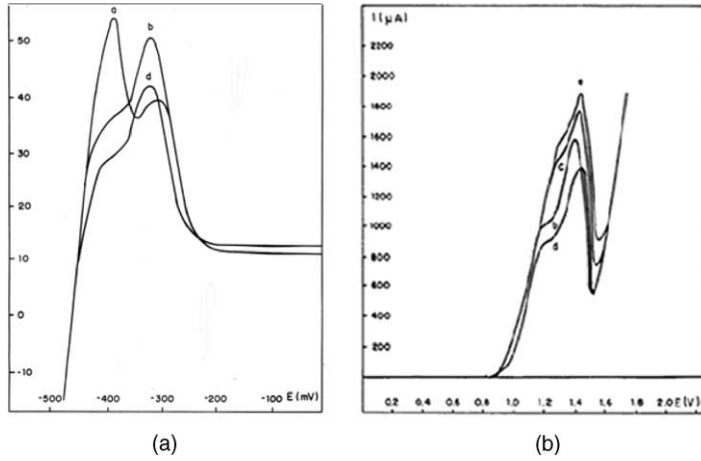
Fig. 3. Potentiodynamic anodic polarisation curves in 0.1 N H$_2$SO$_4$ at a 10 mV/s sweep rate. Panel (a) depicts the complex peak at low potential for the unmodified sample, (curve a) aged for 1000 h at 400 °C, and (curve b) aged for 2000 h at 400 °C (curve d). Panel (b) indicates the complex peak at high potential sample, (curve a) aged for 1000 h at 400 °C, (curve b) aged for 2000 h at 300 °C, (curve c) aged for 2000 h at 400 °C, and (curve d) aged for 1000 h at 300 °C (curve e).
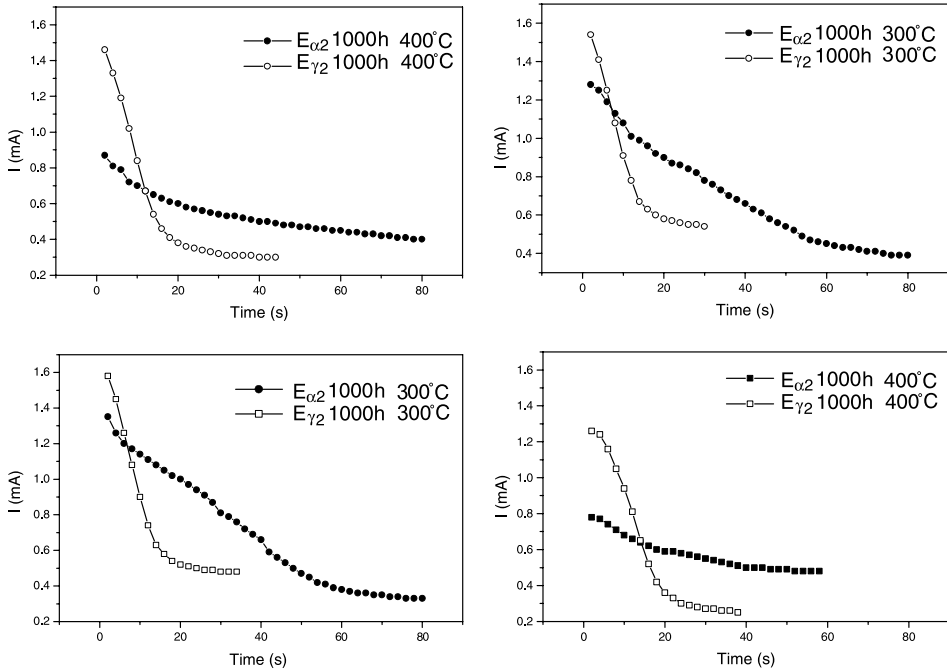
Fig. 4. Chronoamperometry experiment conducted at $E_{2\alpha}$ and $E_{2\gamma}$ potential.

Fig. 3a reveals that the aging treatment decreased the current peak at $E_{1\alpha}$ potential and that the impairment was dependent on the aging time. Moreover, the current peak at $E_{1\gamma}$ increased with the aging treatment, but did not show a direct correlation with the aging time. Therefore, the critical passivation current for the ferrite phase became less pronounced in the complex peak as the aging time increased. On the other hand, the critical passivation current for the austenite phase became more marked in the complex peak as the aging time increased. This effect may be ascribed to the fact that the aging treatment promoted silicon enrichment in the austenite phase and silicon depletion in the ferrite phase. Consequently, the aging treatment caused silicon enrichment of the passivated film in the austenite phase and silicon depletion of the passivated film in the ferrite phase. Silicon enrichment of the surface oxide film was observed by Rhodin [11] on the austenitic microstructure of AISI 304 stainless steel, although he found no chromium or iron enrichment. Rhodin also observed that surface oxide films with silicon are more corrosion resistant and that the distribution of alloy elements in the substrate and the oxide film can differ.

Table 2 indicates how the critical passivation current varied with the duration and temperature of the aging treatment. Evaluating the effects of time and temperature on the critical passivation current for secondary passivation is complex, because it is composed of current dissolution, stoichiometric transformation and oxygen evolution.

Fig. 3 and Table 2 show that the aging treatment strongly influences the passivation of aged DSS, probably due to enrichment of the alloying surface during aging. It is possible that silicon enrichment of the passivated film occurs after a long period of heat treatment, even at low temperatures, because of its greater formation of free energy oxide compared to that of the other reactive elements in solid solution ($\Delta G_{Cr_2O_3} = -147$ kcal/mol and $\Delta G_{SiO_2} = -173$ kcal/mol at 583 °C), and the lower dissociation pressure of silicon compared to that of chromium (10^{-38} atm for Cr and 10^{-43} atm for Si at 583 °C [9]). Furthermore, the greater solubility of silicon in the austenite phase compared to that of Si in the ferrite phase (19.5 at.% Si in austenite and 3.19 at.% Si in ferrite) [10] suggests that silicon enrichment occurs principally in the austenitic phase, with a consequent depletion in the ferrite phase, mainly due to the precipitation of silicon-rich phases such as G phase.

Aging treatments therefore stimulate galvanic corrosion between the ferrite and austenite phases. This effect was demonstrated by the results of weight loss experiments in 0.1 N sulphuric acid at 60 °C, which indicated that the corrosion rate for a

Table 2
Effects of aging treatment time and temperature on critical passivation current

i_c	Variable	
	Time	Temperature
i_c ($E_{1\alpha}$)	Decrease	Low reproducibility
i_c ($E_{1\gamma}$)	Increase	Low reproducibility
i_c ($E_{2\alpha}$)	Decrease	Decrease
i_c ($E_{2\gamma}$)	Decrease	Decrease
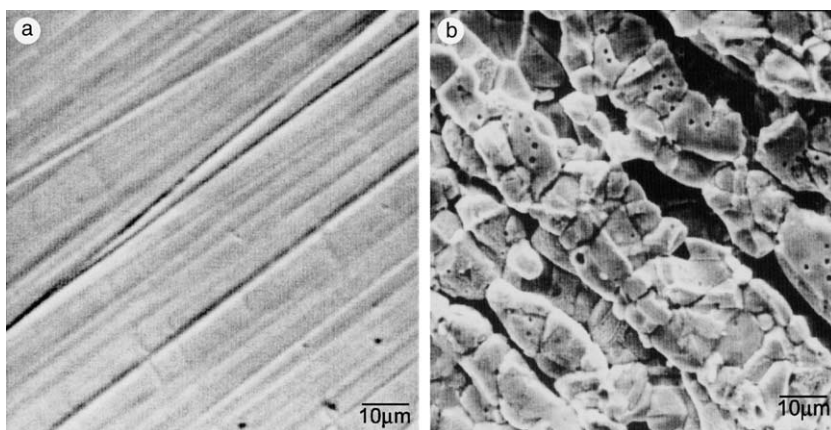
Fig. 5. Surface appearance of aged samples after weight loss experiments in sulphuric acid at 60 °C. (a) 1000 h at 400 °C and (b) 2000 h at 400 °C.

sample aged at 400 °C for 1000 h was 0.23 mpy, remaining unchanged in the un-modified sample, while the corrosion rate of a sample aged at 400 °C for 2000 h was 10.40 mpy. Fig. 5 shows the surface appearance of both samples, viewed by scanning electron microscopy, after the weight loss experiment. These figures reveal sub-stantial corrosion in the sample aged for a longer period.

To obtain additional data about the composition of surface oxide film, as cast and aged samples (2000 h at 400 °C) were subjected to potentiostatic aging at the peak potential ($E_{1\gamma}$ and $E_{2\gamma}$) to facilitate the formation of oxide film over the austenitic phase. The surface film was analysed by XPS, which revealed the presence of chromium oxide (Cr_2O_3), silicon oxide (SiO_2) and iron oxide (Fe_2O_3) in both sam-ples. Table 3 shows a mean value for the austenite and ferrite phases of the atomic Cr/Fe and Si/Fe ratio in the passivated film. These findings indicate that the silicon content in the as cast condition for both potentials was similar, but silicon enrich-ment occurred in the passivated film of the heat-treated sample when aged at $E_{1\gamma}$ potential, i.e., in the austenite phase. The depletion of silicon in the passivated film aged at $E_{2\gamma}$ indicates that silicon participated in the secondary passivation of DSS, occurring due to a complex stoichiometric transformation with simultaneous oxygen

Table 3
Atomic ratio of Cr/Fe and Si/Fe in the passivated film, determined by XPS after 5 min in sulphuric acid at peak potential

	Cr/Fe	Si/Fe
As cast at $E_{1\gamma}$	NA	1.45
Heat treated at $E_{1\gamma}$	0.87	3.00
As cast at $E_{2\gamma}$	0.75	1.53
Heat treated at $E_{2\gamma}$	0.53	0.77

NA: not analysed; heat treated at 300 °C–2000 h.
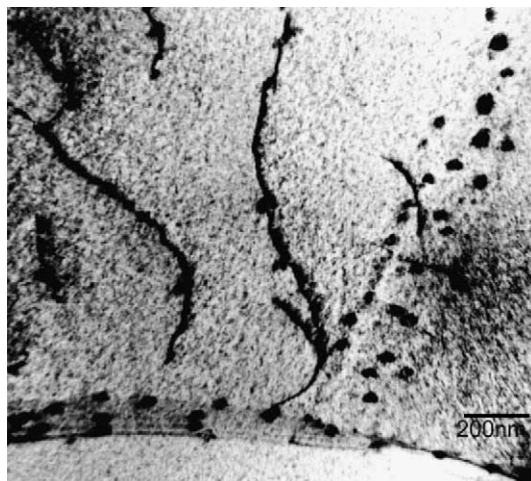
Fig. 6. G phase precipitation and spinodal decomposition occurring in the ferrite phase after aging treatment, identified by TEM.

evolution. No significant variation was observed in the Cr/Fe ratio, indicating the same level of chromium in the passivated film in every condition.

The formation of a surface oxide film in the ferrite phase of aged samples was also influenced by metallurgical transformations that occurred in this phase, namely spinodal decomposition and G phase formation, as depicted in Fig. 6. In both cases, the precipitation of silicon-rich α' and G phases decreased in quantity in solid solution, thus affecting the silicon content of the passivated film in the ferrite phase.

4. Conclusions

1. The passivation of DSSs is affected by long-term aging heat treatment at low temperatures, especially at 400 °C.
2. Long-term aging contributes to silicon enrichment of the passivated film in the austenite phase, with silicon depletion of the passivated film in the ferrite phase.
3. Silicon content influences secondary passivation, which develops more rapidly in the enriched austenite phase than in the depleted ferrite phase.

References

[1] A.M. Irissarri, E. Erauzkin, in: Proceedings of the Fourth European Conference of Advanced Materials and Processes—Euromat 95, Symposium F—Materials and Processing Control, Padua/ Venice, Italy, Sept. 1995, pp. 25–28.
[2] J.H. Potgieter, British Corros. J. 27 (1992) 219.
[3] M.K. Miller, J. Bentley, Mat. Sci. Technol. 6 (1990) 285.
[4] M.E. Wilms, V.J. Gadgil, J.M. Krougman, F.P. Ijsseling, Corros. Sci. 36 (1994) 871.

[5] E. Symniotis, Corrosion 40 (1990) 2.

[6] P.H. Pumphrey, K.N. Akhurst, Mat. Sci. Technol. 6 (1990) 211.

[7] D.A. Shirley, Phys. Rev. B 5 (1972) 4770;
    G.C. Smith, Surface Analysis by Electron Spectroscopy, Plenum Press, NY, 1994.

[8] NACE Basic Corrosion Course, fourth ed., 1973, p. 13.8.

[9] T.B. Massalski, Binary Alloy Phase Diagrams, second ed., ASM Inter., 1992, p. 1771.

[10] S.J. Goodwin, B. Quayle, F.W. Noble, Corrosion 43 (12) (1987) 743.

[11] T.N. Rhodin, Corrosion 12 (1956) 465.